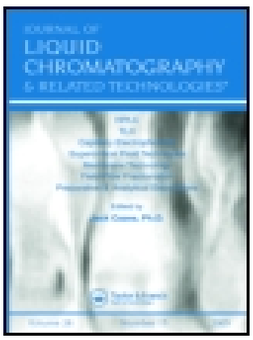

Journal of Liquid Chromatography

ISSN: 0148-3919 (Print) (Online) Journal homepage: http://www.tandfonline.com/loi/ljlc19

Determination of Photodestruction Quantum Yields Using Capillary Electro-Phoresis: Application to o-Phthalalde-Hyde/β-Mercaptoethanol-Labeled Amino Acids

Owe Orwar , Harvey A. Fishman , Mikael Sundahl , Vishal Banthia , Weev Dadoo & Richard N. Zare

To cite this article: Owe Orwar , Harvey A. Fishman , Mikael Sundahl , Vishal Banthia , Weev Dadoo & Richard N. Zare (1995) Determination of Photodestruction Quantum Yields Using Capillary Electro-Phoresis: Application to o-Phthalalde-Hyde/β-Mercaptoethanol-Labeled Amino Acids, Journal of Liquid Chromatography, 18:18-19, 3833-3846, DOI: 10.1080/10826079508014628

To link to this article: http://dx.doi.org/10.1080/10826079508014628

Published online: 23 Sep 2006.

JOURNAL OF LIQUID CHROMATOGRAPHY, 18(18&19), 3833-3846 (1995)

DETERMINATION OF PHOTODESTRUCTION QUANTUM YIELDS USING CAPILLARY ELECTROPHORESIS: APPLICATION TO *o*-PHTHALALDEHYDE/β-MERCAPTOETHANOL-LABELED AMINO ACIDS

OWE ORWAR[1], HARVEY A. FISHMAN[1], MIKAEL SUNDAHL[2], VISHAL BANTHIA[1], RAJEEV DADOO[1], AND RICHARD N. ZARE[1]*

[1]*Department of Chemistry*
Stanford University
Stanford, California 94305-5080
[2]*Department of Organic Chemistry*
Chalmers University of Technology
Göteborg, Sweden

ABSTRACT

Photodestruction quantum yields, Φ_D, were determined for *o*-phthalaldehyde/ß-mercaptoethanol-labeled protein amino acids in aqueous alkaline solution using *trans*-azobenzene actinometry. The Φ_D values ranged from 0.020 to 0.062; the highest were obtained for amide-containing amino acid derivatives (Gln and Asn; Φ_D = 0.062 and 0.054, respectively). The average maximal number of fluorescent photons obtained from the chromophores ranged from 6.4 to 19.0 per molecule. We show that Φ_D values can be determined with the help of an internal standard using capillary electrophoresis with laser-induced fluorescence detection. Generally, good agreement between the Φ_D values obtained in this way and Φ_D values obtained using *trans*-azobenzene actinometry was found. Furthermore, we show that knowledge of the analyte's photochemical properties assists identification of components separated by capillary electrophoresis.

INTRODUCTION

Hjertén (1) was one of the first to demonstrate what he termed "high-performance electrophoresis" by analogy with high-performance liquid chromatography in which

electrophoretic separations were carried out in thin-walled glass tubes of small inner diameter (0.05 to 0.3 mm). Such small glass tubes allowed for efficient heat dissipation so that thermal distortion of the zones was small even at high field strengths. In a classical paper, Jorgenson and Lukacs (2) demonstrated separation efficiencies in excess of 400,000 theoretical plates by performing electrophoresis in capillaries with inner diameters of 75 μm. This methodology is commonly referred to as capillary electrophoresis (CE). Taking full advantage of the high separation efficiencies achieved with CE requires a sensitive and selective detection scheme that does not contribute to any extraneous band broadening. One such scheme is on-line laser-induced fluorescence (LIF) detection (3), but the CE-LIF detection process can be optimized only if several key photophysical and photochemical properties of the analytes are known (4,5). Unfortunately, all the required photophysical and photochemical parameters are not generally known even for derivatives obtained with commonly employed reagents. Another complication of this scheme that has to be taken into account is that separated analytes migrate at different velocities within the CE column and are therefore excited by the laser light for different periods of time (5,6). In this report, we present photodestruction quantum yields (Φ_D) obtained using *trans*-azobenzene actinometry for ten protein amino acids labeled with *o*-phthalaldehyde/ß-mercaptoethanol (OPA/ßME), a reagent used extensively to label protein amino acids for use in liquid chromatography (LC) and CE (7). The fluorescence quantum yields (Φ_f) of these chromophores have been reported (8). It is now feasible to calculate the number of fluorescent photons (n_f) that can be obtained from a single chromophore as described by Hirschfeld (9) and Mathies and coworkers (4) as:

$$n_f = \Phi_f/\Phi_D = k^o_f/k_d \qquad (1)$$

where k^o_f (s^{-1}) is the rate of fluorescence and k_d (s^{-1}) is the rate of photodestruction. Knowledge of n_f is important because it determines the detection sensitivity that can be achieved for a given fluorophore.

Furthermore, we present CE-LIF detection at low and high excitation irradiances of separated standard amino acid derivatives that have equal optical densities. The low-excitation irradiance corresponds to excitation of the chromophores with a few quanta of light, and under these conditions fluorescence intensity, I_f, is proportional to $\Phi_f \tau_t$, where τ_t is the time a molecule is interrogated by the laser beam. The high-excitation irradiance produces complete apparent fluorescence saturation of the chromophores, and under these

conditions I_f is proportional to Φ_f/Φ_D. We show that in the limit of high excitation irradiances, it is feasible to obtain Φ_D values using CE-LIF detection provided that an internal standard with known Φ_f/Φ_D ratio is available to characterize the instrumental response.

MATERIALS AND METHODS

Apparatus

The quantum yields of photodestruction were measured in an optical bench arrangement that consisted of a Xe arc lamp and a monochromator (Applied Photophysics, Leatherhead, UK), as described previously (10). *trans*-Azobenzene (11), calibrated against ferrioxalate (12), was used as an actinometer. The CE experiments in 800-mm long x 67-μm i.d. fused silica capillaries (Polymicro, Phoenix, AZ) were performed using a high-voltage power supply (Glassman, Whitehouse Station, NJ) operated at ~5 to 25 kV. Injections were performed by raising the inlet end of the capillary ~5 cm above the outlet end of the capillary for 30 seconds.

LIF detection in CE experiments was performed using the 325-nm line from a model 4240 NB Liconix He-Cd laser (Santa Clara, CA). An interference filter centered at 325 nm with a 10.5-nm FWHM (Omega Optical, Brattleboro, VT) was used to reject plasma discharge emission and unwanted laser light. The laser beam was focused onto the fused silica capillary using a 50-mm focal-length lens. The beam waist at the focal point ($1/e^2$ intensity) was calculated to be 11 μm. A linear-graded neutral density filter (Melles Griot, Irvine, CA) was used to control excitation laser powers. The detection zone of the capillary, which was produced by stripping off the polyimide layer on a 5-mm length by heating was housed in a parabolic mirror. The fluorescence emission was collected at a right angle with respect to the incident laser beam and focused by a 150-mm focal length plano-convex lens onto the photomultiplier tube (Hamamatsu model R4632, San Jose, CA). The photomultiplier tube was biased at 500 V. The fluorescence emission was filtered to reject Raman and Rayleigh scattered light by a 450-nm notch interference filter (~30 nm FWHM) from Omega Optical. The photomultiplier tube current was amplified by a picoammeter, converted to voltage, and digitized using an analog-to-digital board (Chrom-1, Omega Engineering, Stamford, CT). It was displayed using commercial software (Galactic Industries, Salem, NH) run on a personal computer. Absorbance measurements were performed using a UV-VIS spectrophotometer (model 8450, Hewlett Packard, Palo Alto, CA).

Amino Acids, Reagents, and Derivatization Procedures

10-mM solutions of amino acid standards (Sigma, St. Louis, MO) were prepared in distilled deionized water. A borate buffer for use in CE experiments was prepared from disodiumtetraborate (~11 mM, pH 9.1) (Merck, Darmstadt, Germany). Another borate buffer for use with reagents was prepared by dissolving boric acid in distilled deionized water to a final concentration of 0.4 M. The pH was adjusted to 9.5 with 5.0-M NaOH. The OPA/ßME reagent solutions were prepared by dissolving 100 mg OPA (99%, Sigma) in 1 mL of methanol and adding to this solution 100 μL of ßME (99%). The borate buffer was added to this solution to create a final volume of 10 mL. Derivatizations were performed in polypropylene vials. Reagent-to-standard-volume ratios of 1 : 2 were typically used. In all CE experiments, concentrations of analytes were corrected to give the same absorbance at 325 nm. Determination of photodestruction quantum yields by *trans*-azobenzene actinometry was performed in a 50-mM borate buffer (pH=9) using stoichiometric amounts of reactants. The completion of the reactions was ascertained by absorption measurements at 336 nm.

RESULTS AND DISCUSSION

Table 1 lists several photophysical and photochemical properties of OPA/βME-labeled amino acids. Included are the Φ_D values that we obtained using *trans*-azobenzene actinometry, together with the fluorescence quantum vields (8), and the fluorescence and photodestruction rate constants. The Φ_D values obtained here are similar to previous estimates of the monophotonic photodestruction quantum yields of aromatic amino acids using excitation at 254 nm ($\Phi_{D,\,Trp}$ = 0.9 %; $\Phi_{D,\,Tyr}$ = 2.2 %; $\Phi_{D,\,Phe}$ = 1.9 %) (13). The highest Φ_D values were obtained, however, for the amide-containing chromophores OPA/βME-Asn and OPA/βME-Gln; their Φ_D values are 5.4% and 6.2%, respectively. Earlier studies of OPA/βME-labeled α-peptides correlated high photodestruction quantum yields with the proximity of amide groups to the isoindole moiety (14). Intramolecular electron transfer, in which the isoindole functions as an excited-state electron donor and nearby amide groups function as electron acceptors, may be the mechanism underlying these effects.

Recall that the ratio between the fluorescence quantum yield and the photodestruction quantum yield, Φ_f/Φ_D, determines the average maximum number of fluorescent photons a molecule can yield (4,9). These ratios for the OPA/βME-labeled amino acids are listed in Table 1; note that they are several orders of magnitude lower than those of chromophores

TABLE 1

Photophysical and photochemical properties of *o*-phthalaldehyde/ß-mercaptoethanol-labeled amino acids

AMINO ACID	[a]Φ_f	[b]Φ_D	[c]Φ_f/Φ_D	[d]k_f/s^{-1}	[e]k^o_f/s^{-1}	[f]k_d/s^{-1}
Ala	0.40	0.031*	12.9	5.43×10^7	2.17×10^7	1.68×10^6
Arg	0.40	0.021	19.0	5.13×10^7	2.05×10^7	1.08×10^6
Asn	0.40	0.054	7.41	5.75×10^7	2.30×10^7	3.10×10^6
Asp	0.41	0.031	13.2	5.38×10^7	2.20×10^7	1.67×10^6
Gln	0.40	0.062	6.45	5.40×10^7	2.16×10^7	3.53×10^6
Leu	0.41	0.037	11.1	5.00×10^7	2.05×10^7	1.85×10^6
Ser	0.41	0.037	11.1	5.05×10^7	2.07×10^7	1.87×10^6
Thr	0.36	0.043	8.37	5.24×10^7	1.89×10^7	2.25×10^6
Trp	0.33	0.027	12.2	4.98×10^7	1.64×10^7	1.34×10^6
Tyr	0.33	0.020	16.5	5.00×10^7	1.65×10^7	1.00×10^6
Val	0.34	0.035	9.71	5.00×10^7	1.70×10^7	1.75×10^6

[a]Fluorescence quantum yields (Φ_f) taken from Chen et al. (8).

[b]Photodestruction quantum yields (Φ_D) obtained using *trans*-azobenzene actinometry as described in the experimental section.

[c]The ratio between the fluorescence quantum yield and the photodestruction quantum yield (Φ_f/Φ_D), which equals the maximum number of fluorescent photons that can be obtained for a single chromophore.

[d]The observed rate of fluorescence (k_f) taken from Chen et al. (8).

[e]The rate of fluorescence (k^o_f) was calculated as; $k^o_f = k_f \Phi_f$.

[f]The rate of photodestruction (k_d) was calculated as; $k_d = k_f \Phi_D$.

* Data taken from ref. 10

employed as laser dyes and high-sensitivity fluorescence markers, for example, Rhodamine 6G in ethanolic solution ($\Phi_f/\Phi_D = 1.9 \times 10^6$) (15), Texas Red in ethanolic solution ($\Phi_f/\Phi_D = 1.4 \times 10^6$) (15), and fluorescein in water-based solution ($\Phi_f/\Phi_D = 3.7 \times 10^4$) (16).

As stated, the optimization of LIF detection requires knowledge of certain molecular parameters. For cases in which only singlet saturation and photochemistry are important, an equation that describes the fluorophore behavior has been derived by Mathies and co-workers (4):

$$n_f = (\Phi_f/\Phi_D)[1-\exp\{-k\tau/(k+1)\}] \qquad (2)$$

This function asymptotically approaches Φ_f/Φ_D. For a population of molecules, the fluorescence intensity (I_f) is obtained by multiplying the right side of Eq. 2 by the number

of molecules. The parameters needed to calculate nf for a given excitation irradiance are: Φ_f, Φ_D, and τ, which the last is the ratio of the transit time τ_t (s) to the photodestruction time τ_D (s); and k, which is the ratio between the rate of absorption k_a (s^{-1}) and the observed rate of fluorescence k_f (s^{-1}). Even though different OPA/βME-labeled analytes can be photoionized to different extents in aqueous alkaline solution (10), we assume that analysis using Eq. 2 is sufficient for the chromophores in the present study. This assumption is based on the idea that we are concerned mainly with obtaining a qualitative description of the excitation irradiance dependence for the chromophores. Spectroscopic observations in water-based solutions suggest that triplet absorption is negligible in some OPA/βME amino acid derivatives (10), indole, N-methylindole, and tryptophan (17).

Figure 1 shows plots of calculations using Eq. 2 for the OPA/βME-Ala and OPA/βME-Asn derivatives, which represent two chromophores that have different photodestruction quantum yields but identical fluorescence quantum yields (Table 1). Figure 1 also shows the effect of increasing the transit time for the Ala derivative. Figure 2 shows the laser irradiance dependence for the same two derivatives in a CE experiment in which the analytes (same concentration corresponding to equal optical density at λ_{abs}=325 nm) are detected under identical conditions, that is identical excitation irradiance and transit time. Qualitatively, the results agree well with the calculations shown in Figure 1, which suggest that (1) the rate of photodestruction is the major difference between these two chromophores and (2) that the photophysical constants are similar. The Φ_f/Φ_D value obtained for the Ala derivative in this experiment was 1.99 ± 0.05 (mean ± s.d.) times higher than that for the Asn derivative, which is close to the expected value of 1.74 ± 0.12 (mean ± s.d.). More experiments are shown below that demonstrate how Φ_D values can be obtained in CE-LIF detection experiments for analytes that migrate at different velocities.

In experiments where the laser power dependence was investigated for Asn and Asp labeled with OPA/ethanethiol (OPA/EtSH), a similar result as shown in Figure 2 was obtained (data not shown). The only difference was that the EtSH-containing chromophores yielded slightly lower fluorescence intensities at the highest excitation irradiances. This result is consistent with lower fluorescence quantum yields of the EtSH-labeled analogs (8) and suggests that the photochemical properties of βME- and EtSH-labeled chromophores are similar.

In CE, separated analytes travel through the separation column at different velocities and are therefore interrogated in an on-line LIF detection scheme by the laser beam for different periods of time. With a delta-function detector, this spread in analyte velocities

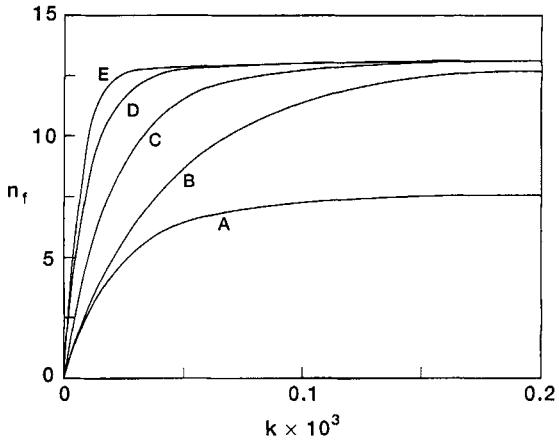

Figure 1.

Fluorescence intensity (n_f) for a single chromophore as a function of normalized excitation intensity k for the OPA/βME-Asn (A) and OPA/βME-Ala derivatives (B). The graphs were constructed using Eq. 2 and the Φ_f and Φ_D values listed in Table 1, a transit time of 23.7 ms, and the photodestruction lifetimes ($1/k_d$, see Table 1) for the respective derivatives. Also shown is the effect of varying the transit time for the Ala derivative (C, τ_t=47.4 ms; D, τ_t=94.8 ms; E, τ_t=142.2 ms).

results in increased temporal widths of the analyte bands in proportion to their migration time (6). Shear et al. (5) previously showed that detection conditions can be optimized for bands moving at different velocities by adjusting the excitation irradiance and the data-digitization rate.

Here we will show quantitatively how this spread in analyte velocities and differences in photochemistry affects the signal output using low- and high-excitation irradiances. At low-excitation irradiances, the fluorescence intensity (I_f) increases linearly according to:

$$I_f \propto K\,\Phi_f\,I_0\tau_t\,A \qquad (I_0 << I_{SAT}) \qquad (3)$$

where K is a constant, I_0 the excitation intensity, and A the absorbance [which equals ε c b, where ε is the molar absorptivity (M^{-1} cm^{-1}), c the concentration (M), and b the optical pathlength (cm) in the detection zone]. We define I_{SAT} to be the level at which $I_f = \Phi_f/2\Phi_D$. In our experiments, the product K I_0 A is kept constant and hence:

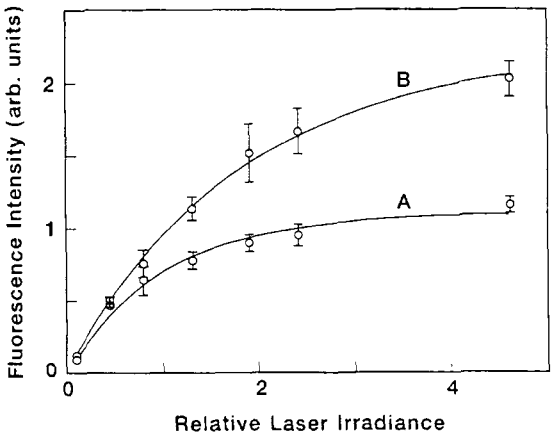

Figure 2.

Fluorescence intensity as a function of relative laser excitation irradiance for the OPA/βME-Asn (A) and OPA/βME-Ala (B) derivatives in CE-LIF detection experiments. Each data point represents the mean ± s.d. (n=3). The solid lines show scaled best-curve-fits to Eq. 2.

$$I_f \propto \Phi_f \tau_t \qquad (I_O << I_{SAT}) \qquad (4)$$

This linear relationship is demonstrated in Figure 3, which shows the results of electrophoresis of the Trp derivative at different velocities and excitation using a low-excitation irradiance ($I_O << I_{SAT}$). This relationship is also shown in the electropherograms in Figure 4a-c, which represent results of four amino acid derivatives (having equal optical density at λ_{abs}=325 nm) traveling at different velocities and excited using low laser irradiance. As presented in Table 2, a good correlation exists between experimentally obtained peak areas in these CE experiments and peak areas calculated using Eq. 4. Figure 4d shows a computer simulation constructed to create gaussian peaks with areas proportional to $\Phi_f \tau_t$ for each derivative. The simulated peaks were centered at the experimentally found migration times for each analyte with a ±3.5 σ basewidth based on the analyte's respective temporal width.

At high laser-excitation irradiance, at which point the fluorescence is saturated,

$$I_f \propto \Phi_f/\Phi_D \qquad (I_O >> I_{SAT}) \qquad (5)$$

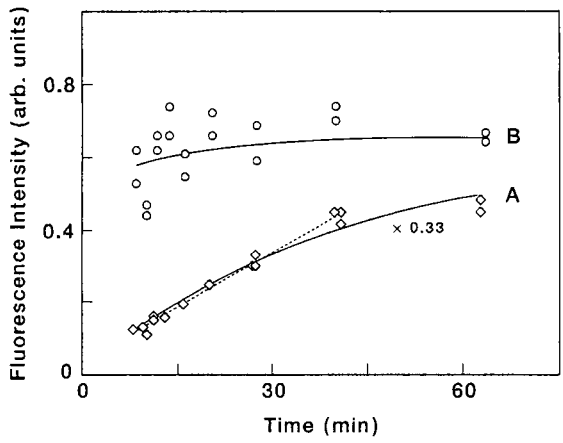

Figure 3.

Fluorescence intensity (peak area measurements) as a function of migration time for the Trp derivative at low (A) and high (B) laser-excitation irradiance. The desired migration times were obtained by adjusting the separation voltage. The dotted line shows a linear curve fit (r=0.9938) to all except the two last data points.

TABLE 2

Comparison between peak areas obtained using capillary electrophoresis with laser-induced fluorescence detection and the calculated product $\Phi_f\tau_t$ for each amino acid derivative at low-excitation irradiance.

Amine	Peak Area (mean ± s.d.; n=3)	[a](Peak Area)$_i$/(Peak Area)$_{Asp}$ (mean ± s.d.)	[b]$(\Phi_f\tau_t)_i/(\Phi_f\tau_t)_{Asp}$ (mean ± s.d.)
Trp	6.53 ± 0.55	0.60 ± 0.06	0.50 ± 0.05
Asn	7.43 ± 0.55	0.69 ± 0.07	0.62 ± 0.06
Ala	7.30 ± 0.75	0.67 ± 0.08	0.64 ± 0.06
Asp	10.83 ± 0.66	1.00 ± 0.09	1.00 ± 0.10

[a]Peak area for each derivative is normalized to that of the Asp derivative.
[b]The product $\Phi_f\tau_t$ for each derivative is normalized to that of the Asp derivative. The Φ_f values used are listed in Table 1 and are assumed to be correct within ± 5% (no estimate of the error was given in ref. 8). τ_t was calculated as $\sqrt{\pi}r/v$, where r is the radius of the laser beam at focus and v the analyte velocity, and was calculated from distributions of retention times to be correct within ± 5 %.

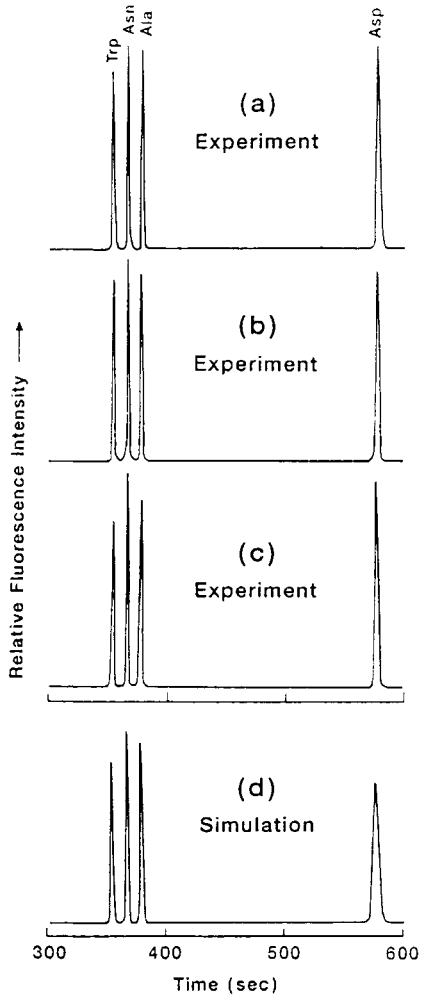

Figure 4.

a-c. Separation of an amino acid standard (Trp, Asn, Ala, and Asp) derivatized with OPA/βME. The concentrations of the amino acid derivatives were adjusted to give the same optical densities at λ_{abs}=325 nm. The derivatives were excited using low-excitation irradiance ($I_0 << I_{SAT}$). The baseline noise obtained in the CE experiments was subtracted using a linear fit.

d. A computer simulation constructed to create gaussian peaks with areas $\propto \Phi_f \tau_t$ for each derivative. The simulated peaks were centered at the experimentally found migration times for each analyte with a ±3.5 σ basewidth based on the analyte's respective temporal width.

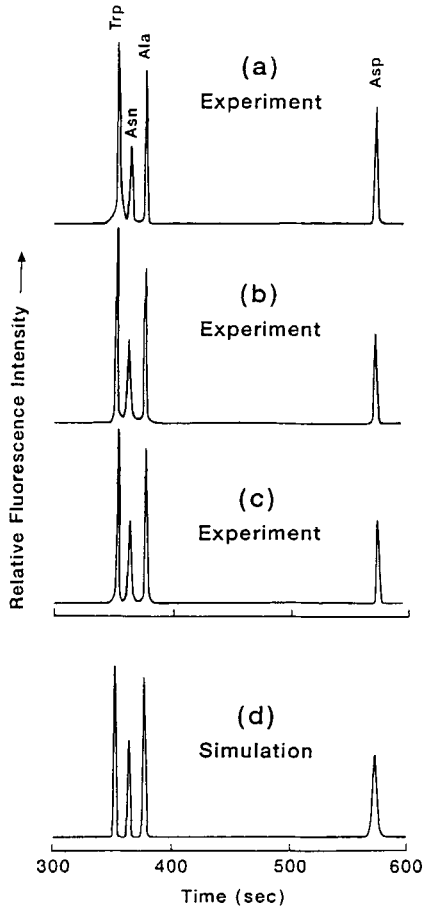

Figure 5

a-c. Same experimental conditions as in Figure 4a-c, except that high-excitation irradiance ($I_0 >> I_{SAT}$) was employed.

d. A computer simulation performed as in Figure 4d, except that it was constructed to create gaussian peaks with areas $\propto \Phi_f/\Phi_D$ for each derivative.

TABLE 3

Comparison between peak areas obtained using capillary electrophoresis with laser-induced fluorescence detection and the calculated ratio Φ_f/Φ_D for each amino acid derivative at high-excitation irradiance.

Amine	Peak Area (mean ± s.d.; n=3)	[a](Peak Area)$_i$/(Peak Area)$_{Asp}$ (mean ± s.d).	[b]$(\Phi_f/\Phi_D)_i/(\Phi_f/\Phi_D)_{Asp}$ (mean ± s.d.)
Trp	250 ± 46	1.03 ± 0.20	0.92 ± 0.09
Asn	106 ± 12	0.44 ± 0.06	0.56 ± 0.06
Ala	243 ± 5.7	1.00 ± 0.06	0.98 ± 0.10
Asp	243 ± 15	1.00 ± 0.09	1.00 ± 0.10

[a]Peak area for each derivative is normalized to that of the Asp derivative.
[b]The ratio Φ_f/Φ_D for each derivative is normalized to that of the Asp derivative.
The Φ_f and Φ_D values used are listed in Table 1. The errors in Φ_f and Φ_D are both estimated to be ±5%.

is predicted from Eq. 2. This relationship was verified experimentally by using high-irradiance excitation in the CE runs presented in Figure 3, which shows the results of electrophoresis of the Trp derivative at different velocities, and in Figure 5a-c, which show separations of the same four derivatives as in Figure 4a-c. Table 3 presents a comparison of the relative peak areas obtained experimentally for each of these derivatives together with the relative peak areas calculated from Eq. 5. By using the Asp derivative as an internal standard with known Φ_f/Φ_D ratio it is straightforward to calculate the Φ_D values for the other three derivatives from the CE-LIF detection experiments from:

$$a_i/a_j=\Phi_{f_i}\Phi_{D_j}/\Phi_{f_j}\Phi_{D_i} \qquad (6)$$

where a_i and a_j are the peak areas, Φ_{f_i} and Φ_{f_j} the fluorescence quantum yields, and Φ_{D_i} and Φ_{D_j} the photodestruction quantum yields of the analyte and the internal standard, respectively. The Φ_D values obtained in this way are 2.4%, 6.9%, and 3.0% for the Trp, Asn, and Ala derivatives, respectively, which generally is in good agreement with the Φ_D values obtained using *trans*-azobenzene actinometry (Table 1). The computer simulation (Fig. 5d) was performed as for Figure 4d, except that is was constructed to create gaussian peaks with areas proportional to Φ_f/Φ_D for each derivative.

The results demonstrate that if Φ_f and Φ_D values of the chromophores are known, peak characterization may be simply determined by performing detection at low excitation irradiance (where I_f increases linearly) and at high excitation irradiance (region where the fluorescence is saturated). Also, Φ_D values may be obtained using CE-LIF detection and the analysis provided by Eq. 2 if a suitable standard with known Φ_f/Φ_D ratio exist. The only requirement is that the Φ_f values of the analytes are known. The advantage of this procedure over that of bulk solution actinometry is that (1) it measures the photodestruction quantum yield of a separated pure product, (2) it is applicable for simultaneous multi-species determination, and (3) it requires only trace quantities of material.

ACKNOWLEDGMENTS

O. Orwar is supported by the Swedish Natural Science Research Council (No. K-PD 10481-301). H. A. Fishman is a W. R. Grace fellow. The authors gratefully acknowledge the help of Dr. Robert Guettler. Supported by grants from the National Institute of Mental Health (MH45423-03 and MH45324-05) and Beckman Instruments, Inc.

REFERENCES

1. S. Hjertén J. Chrom., 270: 1 (1983)
2. J. W. Jorgenson, K. D. Lukacs Anal.Chem., 53: 1298 (1981)
3. E. Gassmann, J. E. Kuo, R. N. Zare, Science, 230: 813 (1985)
4. R. A. Mathies, K. Peck, L. Stryer Anal. Chem., 62: 1786 (1990)
5. J. B. Shear, R. Dadoo, H. A. Fishman, R. H. Scheller, R. N. Zare Anal. Chem., 65: 2977 (1993)
6. X. Huang, W. F. Coleman, R. N. Zare J. Chrom., 480: 95 (1989)
7. M. Albin, R. Weinberger, E. Sapp, S. Moring Anal. Chem., 63: 417 (1991)
8. R. F. Chen, C. Scott, E. Trepman Biochim. Biophys. Acta, 574: 440 (1979)
9. T. Hirschfeld Applied Optics 15: 3135 (1976)
10. O. Orwar, M. Sundahl, M. Sandberg, I. Jacobson, S. Folestad Anal. Chem., 66: 4471 (1994)
11. G. Gauglitz, S. Hubig J. Photochem. 30: 121 (1985)
12. C. G. Hatchard, C. A. Parker Proc. R. Soc. London A, 235: 518 (1956)
13. E. V. Khoroshilova, Y. A. Repeyev, D. N. Nikogosyan J. Photochem. and Photobiol. B., 7: 159 (1990)
14. O. Orwar, S. G. Weber, M. Sandberg, S. Folestad, A. Tivesten, M. Sundahl J. Chrom. 696: 139 (1995)
15. S. A. Soper, H. L. Nutter, R. A. Keller, L. M. Davis, E. B. Shera Photochem. and Photobiol., 57: 972 (1993)

16. R.A Mathies, L. Stryer Single-Molecule Fluorescence Detection: A Feasability Study with β-Phycoerythrin in Applications of Fluorescence in the Biomedical Sciences Allan R. Liss, New York, 1986, pp. 129-140
17. Y. Hirata, N. Murata, Y. Tanioka, N. Mataga J. Phys. Chem., 93: 4527 (1989)

Received: July 10, 1995
Accepted: August 6, 1995